applied sciences

MDPI

Article

Analysis of Dynamic Characteristics of Low-Floor Train Passing Switch in Facing Direction with Bad Alignment Irregularity Ahead of the Turnout

Xiaohong Jia [1,2], Xinwen Yang [3,*] and Guangtian Shi [1,4]

1 School of Mechanical Engineering, Lanzhou Jiaotong University, Lanzhou 730070, China
2 China Railway First Survey and Design Institute Group Co., Ltd., Xi'an 710043, China
3 Shanghai Key Laboratory of Rail Infrastructure Durability and System Safety, Tongji University, Shanghai 201804, China
4 Xi'an Traffic Engineering Institute, Xi'an 710065, China
* Correspondence: xinwenyang@tongji.edu.cn; Tel.: +86-021-69589880

Abstract: A low-floor train–turnout coupling dynamic model considering bad alignment irregularity ahead of the turnout was established on the basis of a field test in which the dynamic performances of a low-floor train passing through a no. 6 turnout in a rail transit depot in China had been measured, as well as the line alignment and wheel and rail profiles. There are two types of wheelsets in the low-floor train: integral wheelset and independent wheelset. The model fully considers the coupling effect between the vehicle and the ballast components, and the simulated results are in consistence with measured results in the field test. Based on this, the influences of train speed, the wheel–rail friction coefficient, and the track alignment optimization of the dynamic performance of low-floor trains passing switch in facing direction are analyzed. The main results indicate that eliminating alignment irregularities before the switch can effectively improve the dynamic performance of the integrated wheelset in the switch and the lateral forces of the outer wheels of these two vehicles are reduced by about 80%, the derailment coefficients are reduced by about 70%, the vertical force is reduced by about 10–20% and wheel load is reduced by approximately 30%.

Keywords: urban rail transit; turnout; low-floor train; alignment irregularity; dynamic characteristics

check for updates

Citation: Jia, X.; Yang, X.; Shi, G. Analysis of Dynamic Characteristics of Low-Floor Train Passing Switch in Facing Direction with Bad Alignment Irregularity Ahead of the Turnout. *Appl. Sci.* **2023**, *13*, 4560. https://doi.org/10.3390/app13074560

Academic Editor: Muhammad Junaid Munir

Received: 28 February 2023
Revised: 26 March 2023
Accepted: 30 March 2023
Published: 4 April 2023

Copyright: © 2023 by the authors. Licensee MDPI, Basel, Switzerland. This article is an open access article distributed under the terms and conditions of the Creative Commons Attribution (CC BY) license (https://creativecommons.org/licenses/by/4.0/).

1. Introduction

The turnout is a railway connection installation which guides the railway vehicles from one track to another. Since the structure of a turnout is complex and various components are involved, for instance, stock rails and blade rails in the switch zone, wing rails, point rails and guard rails in crossing zone, and different joint elements, as a result, the wheel–rail contact in a turnout zone is more complicated, and there are inevitable wheel–rail multiple-point contacts and flange contacts. Such contact behaviors will aggravate the dynamic effect between the vehicle and the turnout, and affect the safety and stability of the train passage. For these reasons, the turnouts, together with the curve lines and rail joints, are known as the three weak parts of the railway track structure [1].

The research on the dynamic performance of vehicles passing the turnouts at home and abroad are mainly through calculations with self-compiled programs, simulations with commercial softwares, and field tests. Based on the vehicle–rail coupling dynamics model of general line and with consideration of the characteristics of the turnout structure, Wang took the lead in establishing a complete vehicle–turnout coupling dynamics model [2], which can describe in detail the main components and the transmission force in the turnout structure, thus reflecting the vibration characteristics more realistically, and he analyzed the influence of the track and vehicle parameters on the vibration of the wheel–turnout coupling system [3]. Ren analyzed the vibration characteristics of the system of trains

passing the turnout in facing the direction on the basis of the vehicle–turnout coupling dynamic model, and proposed an algorithm for calculating wheel flange contact [4,5]. Chen established the vehicle–turnout–bridge coupling dynamic model, and analyzed the vibration responses of the train passing through the turnout on the bridge, which were then verified with an experiment [6]. Schmid focused on the simulation method of a variable profile rail for the blade rail and point rail, and analyzed the dynamic characteristics of a two-axle bogie passing a turnout [7]. Kassa and Nielsen used the multibody dynamics software to establish the vehicle–turnout dynamics model, and analyzed the influence of vehicle speed and passing direction on the dynamic performances of the vehicle, which was then compared with measured results [8]. Pletz used the finite element method to establish the dynamic model of the wheel passing through the crossing and analyzed the influence of axle load, passing speed, passing direction and rail material on the wheel–rail impact forces, equivalent stresses and strains [9]. Alfi and Bruni proposed a mathematical model capable of calculating the dynamic response of the intermediate frequency in a vehicle–turnout coupling system, which considers variable profile rails and elastic tracks, and the correctness of the model was validated by comparison with field-measured data [10]. Xu and Ma [11] analyzed the motion conditions of wheelsets under the same bogie with differential wheelset misalignment based on the mechanical equilibrium condition. Ma and Wang [12] established a model based on the vehicle–turnout coupling system dynamic theory, which was used to analyze the effect of straightening irregularity on vertical wheel–rail force and reduction rate of the wheel load. In addition, they also analyzed the effect of vehicle velocity on the maximum reduction rate of wheel load. Chang and Cai [13] have investigated the effect of various irregularities ahead of the turnout on the dynamic performance of a vehicle at high speeds, based on a random sampling method. Zakeri and Esmaeili [14] developed a numerical model of the train, track, and turnout, and validated it using the data obtained from field measurements conducted in the Iranian Metro network. They investigated the wheel–rail interaction by sensitivity analyses of the heavy vehicle and light track parameters, including train speed, wheel profile, axle load, track gage, and curve radius. Chen and Luo [15] built a finite element model of the track in the frog zone by vehicle–turnout system dynamics considering a variation of rail section and elastic support, bending deformation of turnout sleeper, spacer block and sharing pad effects, and calculated the track integral rigidity distribution in longitudinal direction in the model. Vehicle-turnout rigid–flexible coupling model is built by the finite element method (FEM), multi-body system (MBS) dynamics and Hertz contact theory. Björn [16] presents a parameterized structural track model for the simulation of dynamic vehicle–turnout interaction in a multi-body simulation environment. The model is demonstrated by performing simulations for different vehicle speeds, crossing geometries and fixations between crossing rail and sleepers with different stiffness. In Chiou's study [17], three functions, including the 'V', 'U', and 'S' shapes, are considered for the analysis of the alignment around the turnout in the frog area. The gap between the wing and nose rails is presented as an irregularity function that could be illustrated as a rectangular, single-slope, or double-slope trough model, and the dimension of the wheel of the vehicle are taken into account for the trajectory analysis. The wear and grinding of the nose rail are also demonstrated in detail. The vertical vibrations of the vehicle are simulated as passing through the functional model of the turnout. In Xu's work [18], for a given nominal turnout, several parameterized single harmonic-shaped functions are selected as analytical representations to describe the inherent structural irregularities in a crossing with moveable point, using multi-objective optimization. The objective of the optimization is achieved by ensuring that the responses of the analytical representation applied to a plain track are close to those of the turnout model under the constraint of maximum and minimum wheel–rail contact forces, as well as a correlation coefficient. A plain track with irregularity functions can be considered an equivalent model to enable a fast modeling procedure and an efficient assessment of vehicles. In order to study the dynamic behavior of the light rail vehicle passing through the turnout with a small radius, the typical M + F + T + F + M 5 module

train was selected as the research object. The low-floor train gradually develops from the traditional wheelset to the independent wheelset, but there is a big difference between the two steering abilities. The cases of all traditional wheels and all the independently rotating wheels (IRWs) are selected. Zhou and Chi [19] established the low-floor vehicle train model and the turnout model with variable cross-section based on the multi-point contact method and system dynamics method, and took the China 7th turnout as an example, analyzing the dynamic behavior of the different vehicles, and comparing the difference between the two cases.

This paper is based on a field test of dynamic performance of a low-floor train passing through no. 6 turnout in a rail transit depot of China. Before the turnout there is a reverse curve, and the length of the tangent between the curve and the turnout is rather short. In addition, the test results show that there are bad alignment irregularities at the tangential track. In order to investigate the influence of such abnormal alignment conditions on the dynamic performance of low-floor trains passing through the turnout switch, a corresponding low-floor train–turnout coupling dynamics model is established in a multibody dynamics software, and is validated by comparison with field-measured data. Furthermore, the influences of alignment optimization, different train speed and wheel–rail friction coefficient on the dynamic performance of low-floor trains passing through the switch in facing direction are analyzed utilizing the established model.

2. Field Test and Dynamic Model of Low-Floor Train Passing Switch

2.1. Field Test

In the field test of low-floor trains passing no. 6 switch, there were two test sections at which the wheel–rail contact forces were measured, as shown in Figure 1. Test Section 1 was set at 3500 mm in front of the tip of the switch rail and test Section 2 was set at 100 mm behind the tip of the switch rail.

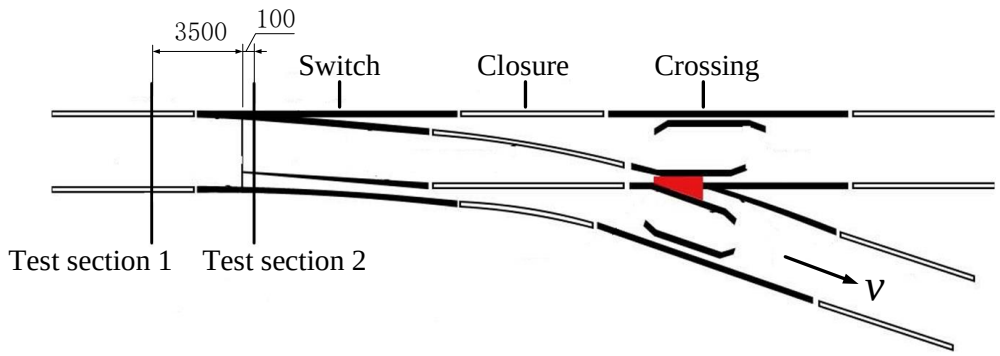


Figure 1. Two test sections of wheel–rail contact forces.

The strain gauges were applied on the rail waist at two sections (Figure 2). The wheel–rail vertical and lateral forces were measured by a full-bridge test. During the test, the vibration data acquisition of the train passing through each test point began at 10 s before the train passed the test point. The DH5920 data acquisition instrument was utilized to synchronously collect data of each test point, with the sampling frequency of 5000 Hz. At 10 s after the train passed by the test point, the data acquisition stopped, and the collected data were recorded as the test data of a single passage. There were 15 passages in total. Subsequently, the test data were processed in MATLAB so as to obtain the effective values of wheel–rail vertical and lateral forces under the action of each wheel axle. The strain gauges for testing the lateral force in Figure 2 shall be affixed to two cross sections 110 mm from the center line of the sleeper box and 20 mm from the bottom edge of the rail. Four strain gauges shall be affixed to the upper surface of the rail bottom, and the direction of the strain gauges shall be at a 45° angle to the longitudinal direction of the rail. The horizontal force to form two bridges was tested according to the upper surface of the rail bottom. After the stress changes are affixed to the rail waist, it is necessary to calibrate it.

The main method is to level the two strain gauge channels, respectively, and apply equally spaced horizontal forces to the rail in the middle of the two patch sections (the center of the sleeper box), to convert the ratio.



(**a**) (**b**)

Figure 2. Field test of low-floor trains passing n. 6 turnout: (**a**) The general test configuration; (**b**) the strain gauges applied on the rail waist.

2.2. Coupling Dynamic Model of Low-Floor Trains and Turnout Switch

In the test, a 70% low-floor train was adopted. The vehicle–track coupling dynamics model was constructed with the help of multi-body dynamics software, UM9.1.1.0. The rail profiles were measured in the test and imported into UM. A basic module of the train consists of two motor vehicles and one trailer vehicle (Figure 3). A motor vehicle in Figure 4a includes one carbody, one bogie, four axle boxes, two integrated wheelsets, and suspension devices. A trailer vehicle in Figure 4b has the same parts as motor vehicle except for the two independently rotating wheelsets. In Figure 4, the red, green and blue lines show longitudinal, horizontal and vertical orientations, respectively. The low-floor vehicle used in the field test contains two modules (i.e., six vehicles in total), and a corresponding model was established in UM, as shown in Figure 5. There are a total of 24 wheels of the two modules, of which the treads were measured by the WS2016-3W-LFT wheel tread measuring instrument. The motor and trailing bogies have the same wheel profiles. The main parameters of the dynamic model are listed in Table 1.

Table 1. Main parameters of dynamics model.

Parameters	Motor Vehicle	Trailer Vehicle
Wheelset mass/kg	1500	560 (Single wheel)
Bogie mass/kg	2970	1971
Carbody mass/kg	18	6.6
Wheel radius/m	0.33	0.33
Wheel base/m	1.492	1.492
Primary longitudinal stiffness/(N·m^{-1})	4×10^6	4.5×10^6
Primary lateral stiffness/(N·m^{-1})	4×10^6	4.5×10^6
Primary vertical stiffness/(N·m^{-1})	8.9×10^5	7.46×10^5
Primary longitudinal damping/(N·s/m)	5000	5000
Primary lateral damping/(N·s/m)	5000	5000
Primary vertical damping/(N·s/m)	10,000	10,000
Secondary longitudinal stiffness/(N·m^{-1})	1.2×10^6	1.2×10^6
Secondary lateral stiffness/(N·m^{-1})	1.2×10^6	1.2×10^6
Secondary vertical stiffness/(N·m^{-1})	4.5×10^5	6.1×10^5
Secondary longitudinal damping/(N·s/m)	1000	1000
Secondary lateral damping/(N·s/m)	1000	1000
Secondary vertical damping/(N·s/m)	2000	2000

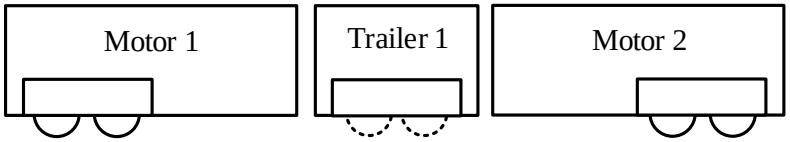
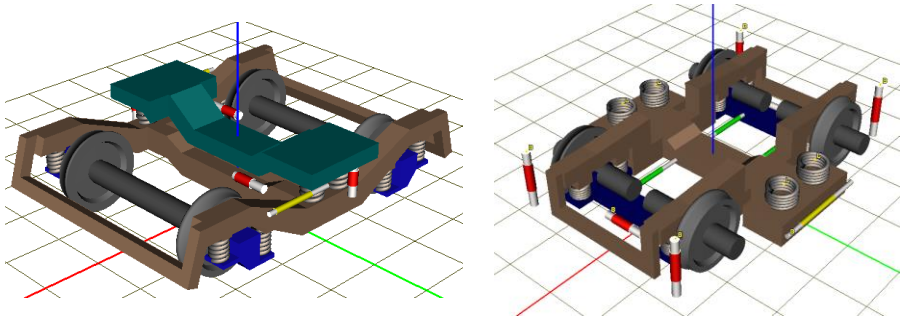


Figure 3. A basic module of a 70% low-floor train.



(**a**) (**b**)

Figure 4. Two types of bogie models: (**a**) a bogie with integrated wheelsets; (**b**) a bogie with the independently rotating wheelsets.



Figure 5. The MBS dynamic model of the two-module low-floor train.

To investigate the dynamic performance of low-floor trains passing the turnout switch in facing direction based on the vehicle–track coupled dynamics theory [20], the left (outer) rails in the switch of the no. 6 turnout (stock rail and blade rail) were treated as variable profile rails in the MBS dynamic software, while the right (inner) rail and the closure rails were treated as a constant profile rail (50 kg/m rail). For the stock rail and blade rail, 15 profiles were measured, as shown in Figure 6. The FASTSIM method was employed to solve the wheel–rail contact relationship.

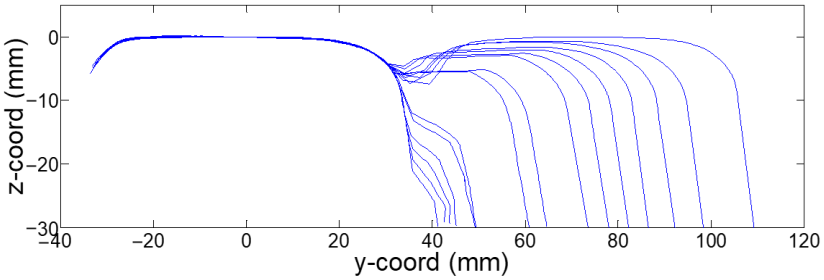


Figure 6. The 15 measured profiles of stock and blade rails.

The plane and vertical sections of the line were mapped by a total station, as shown in Figure 7a. It should be noticed that there is a reverse curve in the line before the turnout, of which the radius is 50 m. After the reverse curve, there is a 1.2 m long tangent, which connects the reverse and the turnout. In addition, by amplifying the measured data at the tangent, it can be observed that it is not an ideal straight line, but a fold line bent towards the inside of the line (Figure 7b), in which the maximum internal shift distance is 10 mm and geometrical difference between the measured and ideal irregularity along the x-coordinate were shown in Figure 7c. Considering that the length of the tangent is rather short and there is alignment irregularity in the tangent, the dynamic performance of the

train will inevitably deteriorate when passing through the tangent in such an abnormal state, which will accumulate until the train enters the turnout, thus leading to detrimental influence on the dynamic performance of the train in the turnout switch.

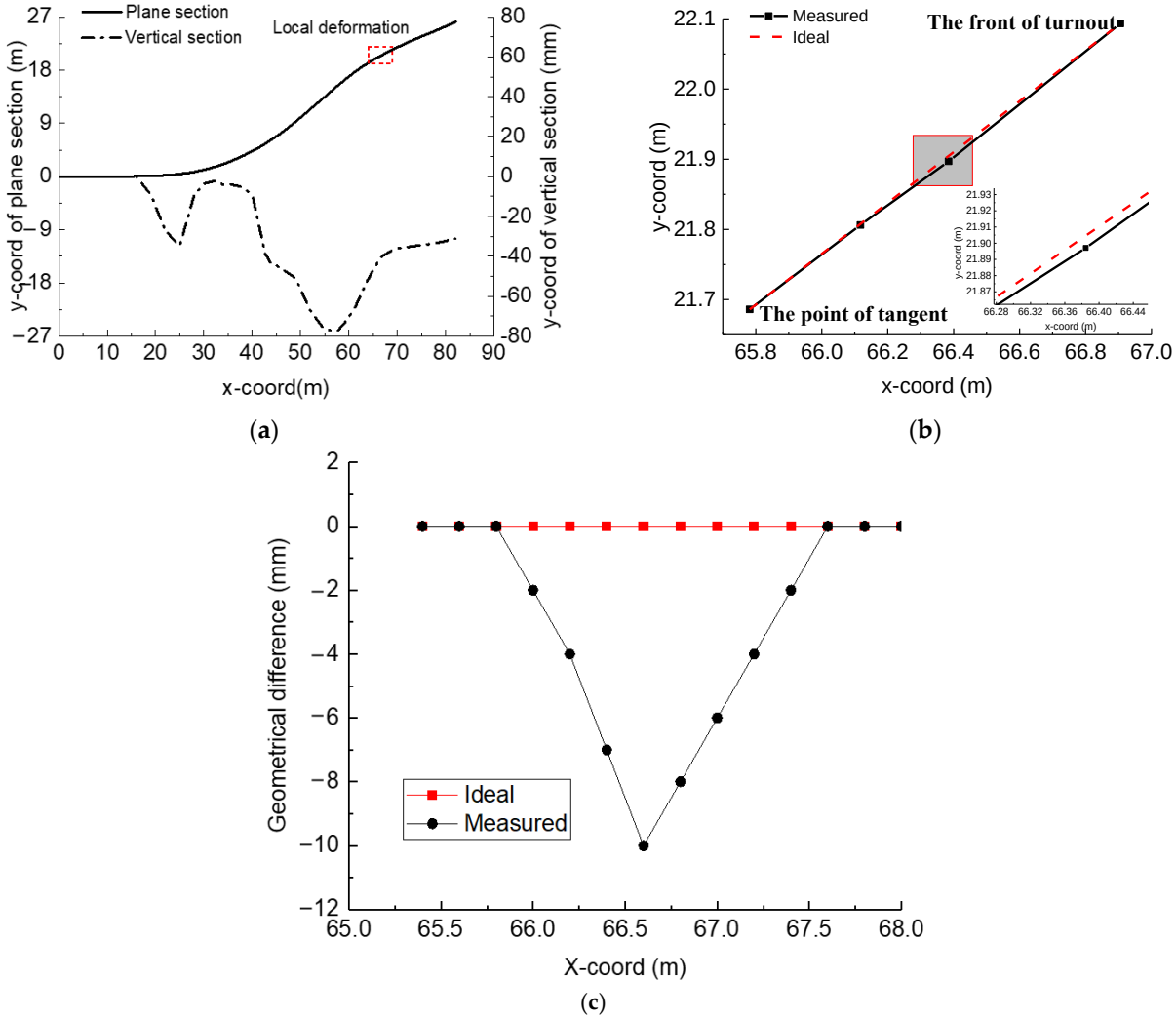


Figure 7. Measured line alignment: (**a**) plane and vertical sections of the line; (**b**) the alignment irregularity on the tangent; (**c**) geometrical difference between the measured and ideal irregularity along the x-coordinate.

3. Model Validation

Using the established model, the dynamic performances of the low-floor train passing through the no. 6 turnout in facing direction were calculated. The speed took 5 km·h^{-1} and the wheel–rail friction coefficient was 0.25. Figure 8 shows the calculated wheel–rail lateral force and vertical force of the outer leading wheel of motor 1 and trailer 1.

It can be seen from Figure 8 that the lateral and vertical forces of the outer trailer leading wheel are greater than those of the outer motor leading wheel when passing through the first curve of the reverse curve, while smaller in the second-stage curve; and the vertical force of the outer motor leading wheel change as the line alignment changes, but that of the trailer wheel only changes in the rightward curve, which is because the independently rotating wheelset does not have the ability to remain in the center position, even if it still remains in flange contact with the left or right track in a tangent. After passing through the reverse curve, the wheel enters the tangent with alignment irregularity, seeing a severe wheel–rail impact at about 72 m, resulting in a sharp increase in wheel–rail contact force which fluctuates violently. The peak values of the wheel–rail lateral force are 34 kN

and 39.7 kN for motor vehicle and trailer vehicle, respectively, and the peak values of the wheel–rail vertical force are 49.2 kN and 44.6 kN, respectively. After entering the turnout switch (the point of blade rail located at 73 m), the fluctuation of the wheel–rail contact force still maintains, but the amplitude decreases with the increasing distance from the blade rail top.

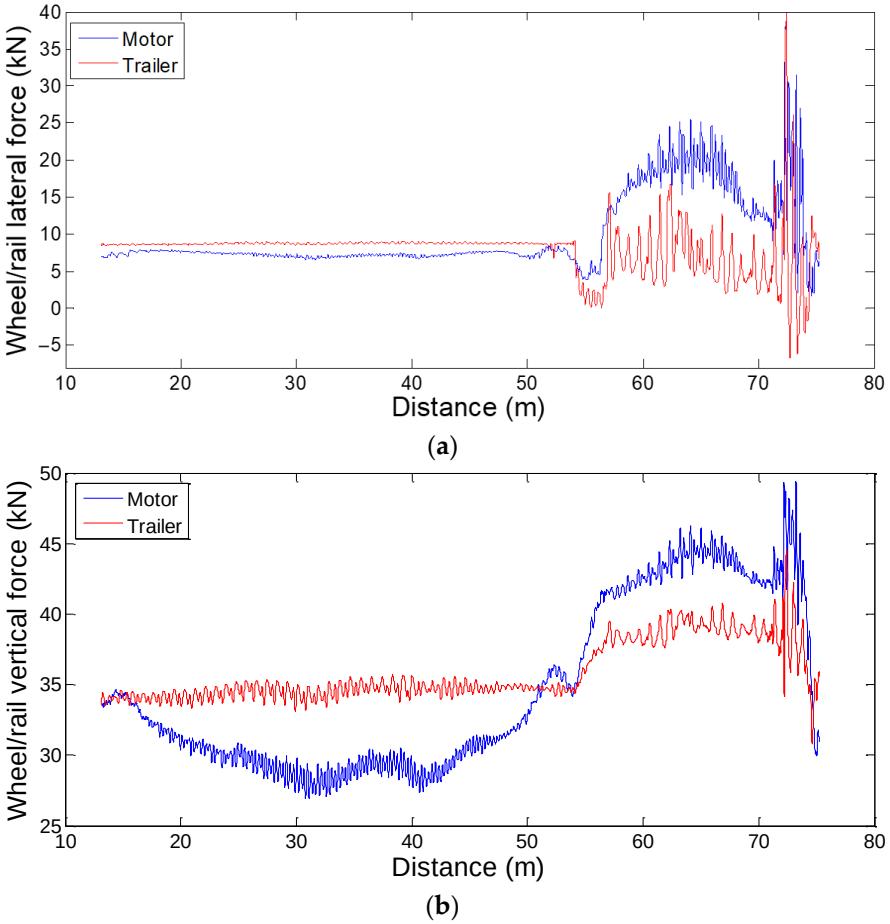


Figure 8. Wheel–rail contact forces of outer leading wheel of motor 1 and trailer 1: (**a**) wheel–rail lateral force; (**b**) wheel–rail vertical force.

Figures 9 and 10 show the measured and simulated root mean square values of the vertical and lateral forces of the 12 outer wheels at Section 1 and Section 2, respectively. It can be seen that the simulated vertical forces are smaller than the measured value in general, and the fit between the measured vertical forces and the simulated ones at Section 2 (in the switch) is better than that at Section 1 (before the switch), especially in the first six wheels. The maximum values of wheel–rail forces on Section 1 and Section 2 are taken from Figures 9 and 10, and the relative error is obtained (as shown in Table 2). The simulation of lateral forces and the measured results are also in good agreement in terms of the trend and values. Thus, the calculation results of the established simulation model are of high reliability.

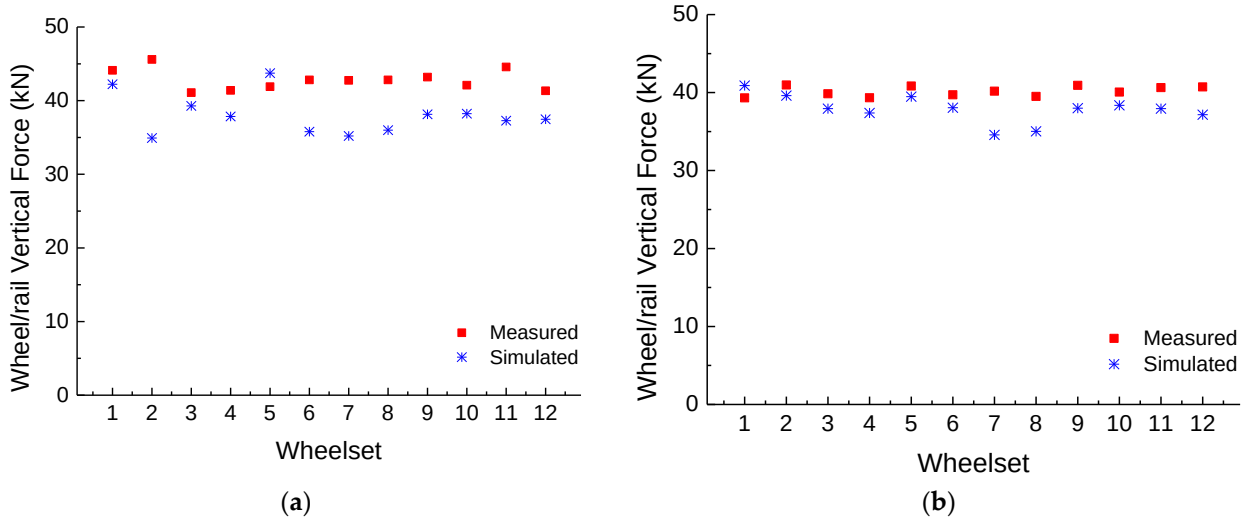


Figure 9. The root mean square value comparison of wheel–rail vertical force of outer wheel: (**a**) vertical force values at Section 1; (**b**) vertical force values at Section 2.

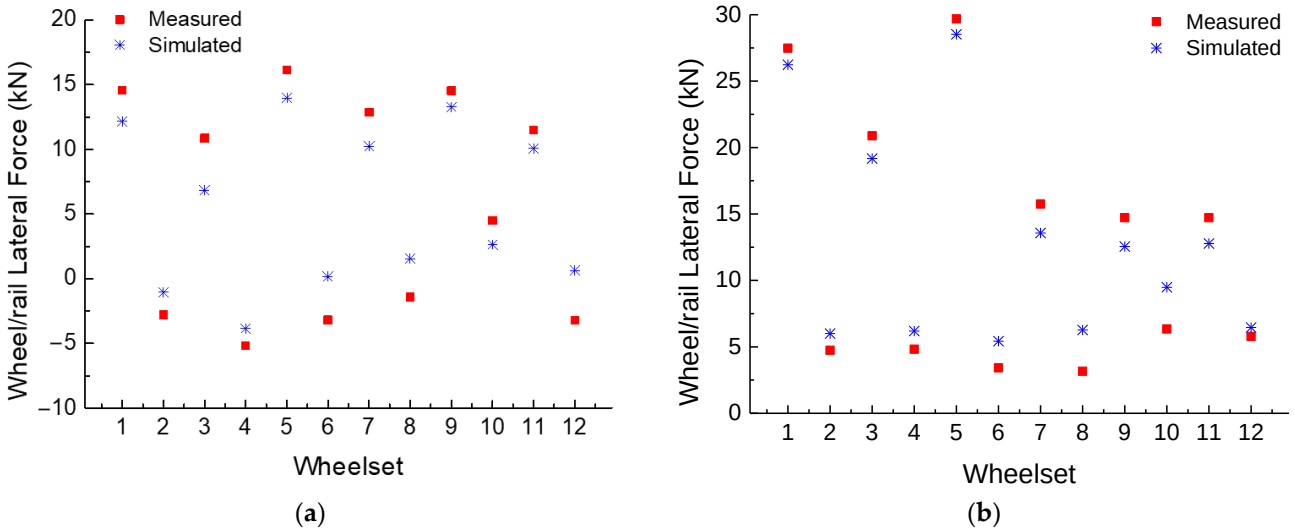


Figure 10. The root mean square value comparison of the wheel–rail lateral force of the outer wheel: (**a**) lateral force values at Section 1; (**b**) lateral force values at Section 2.

Table 2. The maximum error between simulated and measured values.

Wheel–Rail Force	Relative Error/%	
	Section 1	Section 2
Vertical force	8.43	4.29
Lateral force	5.14	5.78

4. Analysis of Influence Factors

The influence of the train speed, wheel–rail friction coefficient and line alignment optimization on the dynamic performance of the low-floor train passing through the switch area is analyzed with the established coupled dynamic model. In each analysis, the parameter condition in the model validation is taken as the basic condition, of which the calculated results are then compared with those of other conditions where a certain influence factor varies. The calculated results include the root mean square values of magnitudes of wheel–rail contact forces, derailment coefficient (Nadal criterion) and the

wheel load reduction rate of the outer leading wheel of motor 1 and trailer 1 (i.e., wheelset 1 and wheelset 3) in the process of the train passing the tangent with alignment irregularities and the switch, respectively.

4.1. Train Speed

The simulated results under the conditions of a train speed at 5 km·h^{-1} (basic speed), 7.5 km·h^{-1}, 10 km·h^{-1}, 12.5 km·h^{-1} and 15 km·h^{-1} are shown in Figure 11.

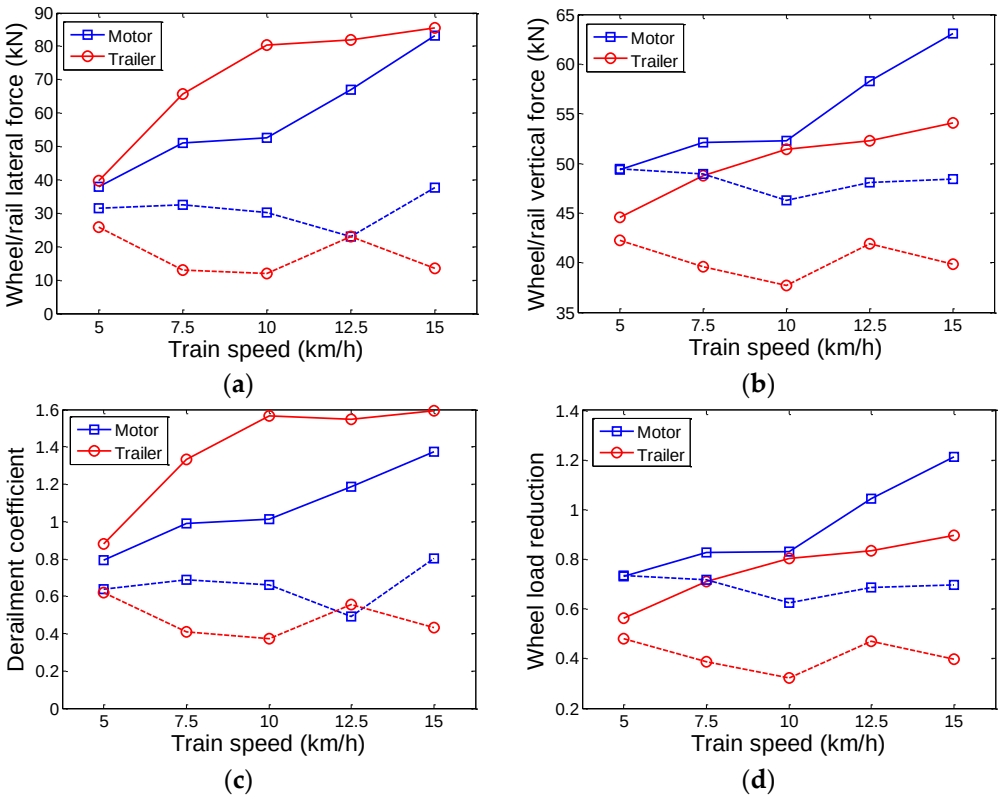


Figure 11. Dynamic characteristics of a train passing the tangent and switch under different train speeds. (**a**) Wheel–rail lateral force; (**b**) wheel–rail vertical force; (**c**) derailment coefficient; (**d**) wheel load reduction; (—) magnitudes in the tangent; (--) magnitudes in the switch.

As seen in Figure 11, in general, since there are alignment irregularities on the tangent before the switch, the wheel–rail relationship just begins to deteriorate at this part, and the magnitudes of the wheel–rail contact forces on the tangent are higher than those of the switch zone. Alongside that, the variation of train speed has a significant influence on the dynamic performance of the train passing through the tangent and switch. The existence of alignment irregularities in the direction leads to a higher possibility of derailment under a respectively small train speed. In detail, the wheel–rail lateral forces of the outer leading wheels of the motor and the trailer increase with the increase in the vehicle speed in the tangent before the switch, but the increase rate is different, as the lateral force of the trailer wheel (independently rotating wheelset) grows faster under the respectively low train speed, and becomes gentle with higher train speeds, while the lateral force of the motor wheel (integrated wheelset) increases gently under low train speeds and faster under high train speeds. After entering the switch, the lateral forces of the motor and trailer wheel are smaller than those in the tangent, and the lateral force of the motor wheel slowly decreases before the speed of 12.5 km·h^{-1}, while the lateral force of the trailer wheel decreases first and then increases. After the speed of 12.5 km·h^{-1}, the lateral force of the motor wheel starts to increase while that of the trailer wheel decreases. The derailment coefficient sees the same trend as the wheel–rail lateral force. As for the wheel–rail vertical force, the vertical force of the trailer wheel is smaller than that of the motor wheel, whether in the tangent

or in the switch zone, which is mainly because the axle load of the trailer is respectively light, at about one third of motor axle load. The variation trends of the vertical force of the motor and the trailer in the tangent and the switch zone are the same as the trends of the lateral force in the corresponding position, but the turning point of the vertical force variation of the motor is earlier at the speed of 10 km·h^{-1}. The variation trend of the wheel load reduction is consistent with that of the vertical force. When there is bad alignment irregularity in the tangent before the turnout, the wheel–rail dynamic performance in the tangent is worse than that in the switch; the dynamic indexes of the integrated wheelset and the independently rotating wheelset increase with the train speed increasing, but at different increase rates. In the switch, the dynamic indexes of the integrated wheelset decrease first and then increase with the increase in speed, while those of the independently rotating wheelset first decrease, then increase and eventually decrease.

4.2. Wheel–Rail Friction Coefficient

The alignment irregularities in the tangent before the switch cause abnormal wheel–rail, aggravating the wheel–rail dynamic effect, leading to the severe wear of rail surface, which results in a large variation in the wheel–rail friction coefficient. Subsequently, the increase in friction will also influence the wheel–rail contact state, affecting the safety of the train passing switch. The magnitudes of simulated results under the wheel–rail friction coefficient 0.10, 0.175, 0.25 (basic friction), 0.325 and 0.40 are shown in Figure 12. It should be noted that in this paper, the wheel–rail friction coefficient refers to the friction coefficient of both the rail top and gauge angle of the stock rail and the blade rail.

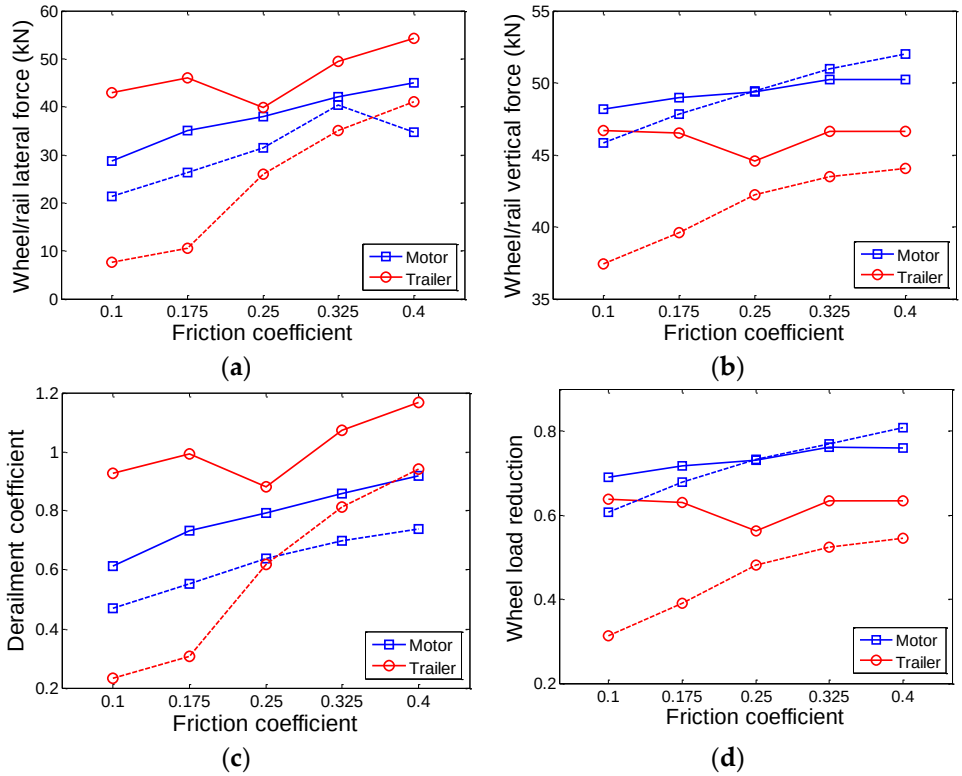


Figure 12. Dynamic characteristics of the train passing the tangent and switch under different friction coefficients. (**a**) Wheel–rail lateral force; (**b**) wheel–rail vertical force; (**c**) derailment coefficient; (**d**) wheel load reduction; (—) magnitudes in the tangent; (--) magnitudes in the switch.

As seen in Figure 12, similarly due to the alignment irregularities in the tangent before the switch, the wheel–rail contact forces in the tangent are greater than those in the switch. In terms of wheel–rail lateral force, the general trend is that the lateral forces of the motor and trailer wheel, in both the tangent and switch, increase with the increase in the friction

coefficient. In particular, the lateral force of the trailer wheel on the tangent declines at the friction coefficient 0.25, and then rises again. Moreover, the lateral force of the trailer wheel in the switch zone increases rapidly with the friction coefficient increasing from 0.175 to 0.4, which suggests that the independently rotating wheelset is more sensitive to the variation of the wheel–rail friction in the switch zone than the integrated wheelset. As for the vertical force, it also tends to increase with the increase in the friction coefficient, and the vertical force of the trailer wheel also declines at the friction coefficient of 0.25 on the tangent. The vertical force of the motor wheel in the switch zone exceeds that in the tangent as the friction coefficient increases. The variation trends of the derailment coefficient and wheel load reduction are inconsistent with trends of the lateral force and vertical force, respectively. It can be concluded that the dynamic indexes of the integrated wheelset in the tangent with alignment irregularity increase with the increase in the friction coefficient, while the dynamic indexes of the independently rotating wheelset will increase both under the condition of smaller and larger friction coefficient, but tend to decrease under the intermediate friction coefficient. In the switch, the dynamic indexes of both wheelsets increase as the friction coefficient increases, and the lateral force and derailment coefficient of the independently rotating wheelset increases remarkably.

4.3. Alignment Adjustment

As analyzed above, in the field test and simulation calculation, the abnormal track alignment in the tangent between the reverse curve and the turnout causes severe wheel–rail impact before entering the switch. The adjustment amount of the alignment irregularities ahead of the turnout is eliminated, and the simulation results of the optimized alignment are compared with the results under basic conditions, presented in Figure 13.

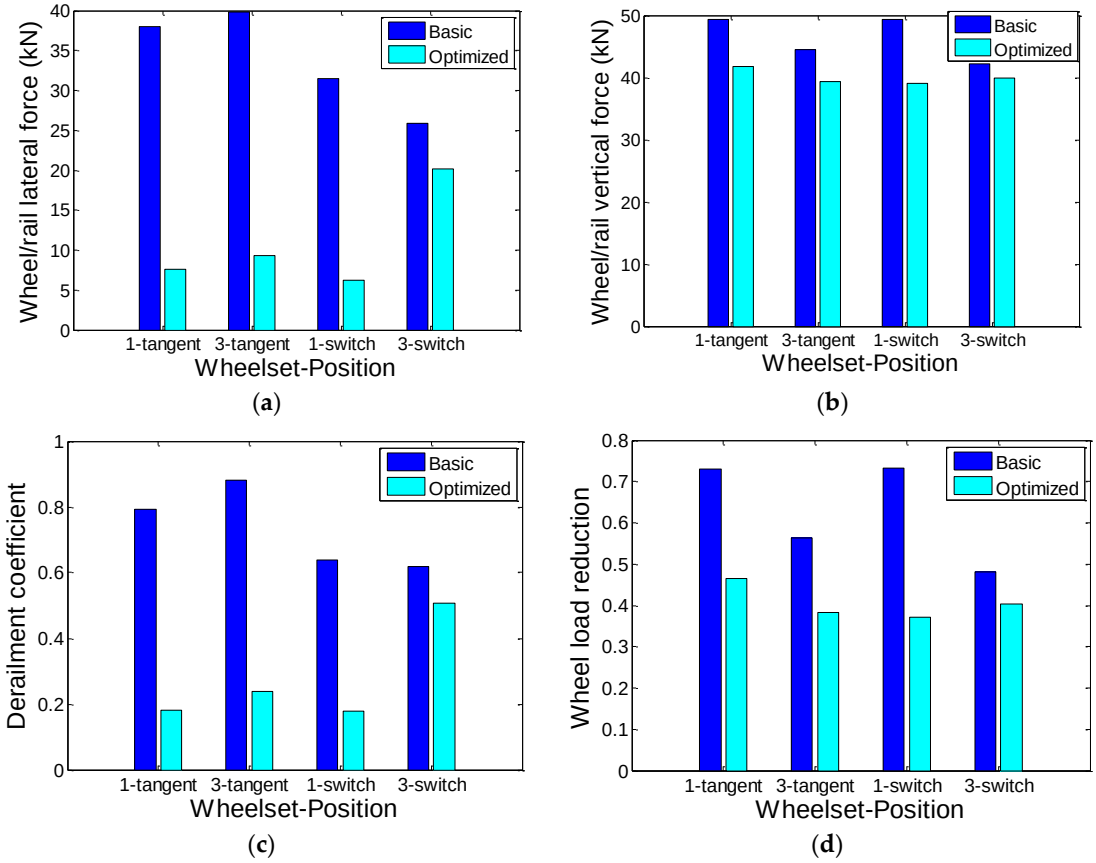


Figure 13. Dynamic characteristics of the train passing the tangent and switch under different track alignments. (**a**) Wheel–rail lateral force; (**b**) wheel–rail vertical force; (**c**) derailment coefficient; (**d**) wheel load reduction.

In Figure 13, it can be seen that eliminating the alignment irregularity before the turnout significantly promotes the dynamic performance of the motor and the trailer passing the tangent. The lateral forces of the outer wheels of these two vehicles are reduced by about 80%, the derailment coefficients are reduced by about 70%, the vertical force reduced by about 10–20% and the wheel load is reduced by approximately 30%. After entering the switch zone, the dynamic performances of the motor have equal promotion as in the tangent. However, the dynamic performance of the trailer is rather limited, which is mainly due to the failure for the independently rotating wheelset to keep in the center position, thus even though the alignment irregularity has been eliminated, the outer leading wheel of the independently rotating wheel is still in flange contact with the outer rail before entering the switch, and with the evolution of the blade rail profile, the wheel–rail impact is still severe. It can be concluded that eliminating alignment irregularities before the switch can effectively improve the dynamic performance of the integrated wheelset in the switch. Due to keeping in flange contact with the outer rail entering the switch, the independent wheelset has a rather limited promotion in dynamic performance when passing the switch.

5. Conclusions and Future Work

In this paper, on the basis of the field test in which the dynamic performances of the low-floor train passing the no. 6 switch in the rail transit depot, the track alignment, wheel treads and rail profiles were measured, and a corresponding low-floor train–turnout switch coupling dynamic model considering the alignment irregularity ahead of the switch was established. The model takes the coupling effect of the train and turnout into full consideration, and the simulated results were validated with measured results. On this basis, the influences of the train speed, wheel–rail friction coefficient and alignment optimization on the dynamic performance of low-floor trains passing the turnout switch were investigated. The results show that:

(1) When there is bad alignment irregularity in the tangent before the turnout, the wheel–rail dynamic performance in the tangent is worse than that in the switch; the dynamic indexes of the integrated wheelset and the independently rotating wheelset increase with the train speed increasing, but at different increase rates. In the switch, the dynamic indexes of the integrated wheelset decrease first and then increase with the increase in speed, while those of independently rotating wheelset first decrease, then increase and eventually decrease.

(2) The dynamic indexes of the integrated wheelset in the tangent with alignment irregularity increase with the increase in the friction coefficient, while the dynamic indexes of the independently rotating wheelset will increase both under the condition of smaller and larger friction coefficients, but tend to decrease under an intermediate friction coefficient. The vertical force of the motor wheel in the switch zone exceeds that in the tangent as the friction coefficient increases. The variation trends of the derailment coefficient and wheel load reduction are inconsistent with the trends of the lateral force and vertical force, respectively. In the switch, the dynamic indexes of both wheelsets increase as the friction coefficient increases, and the lateral force and derailment coefficient of the independently rotating wheelset increase remarkably.

(3) Eliminating alignment irregularities before the switch can effectively improve the dynamic performance of the integrated wheelset in the switch, and the lateral forces of the outer wheels of these two vehicles are reduced by about 80%, the derailment coefficients are reduced by about 70%, the vertical force reduced by about 10–20% and the wheel load is reduced by approximately 30%. Due to keeping in flange contact with the outer rail entering the switch, the independent wheelset has a rather limited promotion in dynamic performance when passing the switch.

Author Contributions: Conceptualization, X.J. and X.Y.; methodology, X.J.; software, X.J.; validation, X.J., X.Y. and G.S.; formal analysis, X.J. and X.Y.; investigation, X.J.; resources, X.Y.; data curation, X.J. and X.Y.; writing—original draft preparation, X.J., X.Y. and G.S.; writing—review and editing, X.J., X.Y. and G.S.; visualization, X.J.; supervision, X.J.; project administration, X.Y. and G.S.; funding acquisition, X.J., X.Y. and G.S. All authors have read and agreed to the published version of the manuscript.

Funding: This research was funded by the National Natural Science Foundation of China, grant number 51778484.

Institutional Review Board Statement: Not applicable.

Informed Consent Statement: Not applicable.

Data Availability Statement: Data are contained within the article.

Conflicts of Interest: The authors declare no conflict of interest.

References

1. Li, C.H. *Railway Track*; Southwest Jiaotong University Press: Chengdu, China, 2012.
2. Wang, P. A Spatial Coupling Model for Railway Turnouts and Its Application. *J. Southwest Jiaotong Univ.* **1998**, *33*, 284–289.
3. Wang, P. A Study on Variation Regularity of Wheel Load on Switch of Turnout. *J. Southwest Jiaotong Univ.* **1999**, *5*, 550–553.
4. Ren, Z. Multi-Point Contact of the high-Speed vehicle-Turnout system dynamics. *Chin. J. Mech. Eng.* **2013**, *26*, 518–525. [CrossRef]
5. Ren, Z.; Sun, S.G.; Xie, G. A method to determine the two-Point contact zone and transfer of wheel-Rail forces in a turnout. *Veh. Syst. Dyn.* **2010**, *48*, 1115–1133. [CrossRef]
6. Chen, R. Theory and Application of Vehicle-Turnout-Bridge Coupling Vibration in High Speed Railway. Ph.D. Thesis, Southwest Jiaotong University, Chengdu, China, 2009.
7. Schmid, R.; Endlicher, K.O.; Lugner, P. Computer-Simulation of the dynamical behavior of a railway-Bogie passing a switch. *Veh. Syst. Dyn.* **1994**, *23*, 481–499. [CrossRef]
8. Elias, K.; Nielsen, J.O. Dynamic interaction between train and railway turnout: Full-Scale field test and validation of simulation models. *Veh. Syst. Dyn.* **2008**, *46*, 521–534.
9. Pletz, M.; Daves, W.; Ossberger, H. A wheel passing a crossing nose: Dynamic analysis under high axle loads using finite element modelling. *Proc. Inst. Mech. Eng. Part F J. Rail Rapid Transit* **2012**, *226*, 603–611. [CrossRef]
10. Alfi, S.; Bruni, S. Mathematical modelling of train–Turnout interaction. *Veh. Syst. Dyn.* **2009**, *47*, 551–574. [CrossRef]
11. Xu, J.; Ma, Q.; Wang, X.; Chen, J.; Chen, R.; Wang, P.; Wei, X. Investigation on the motion conditions and dynamic interaction of vehicle and turnout due to differential wheelset misalignment. *Veh. Syst. Dyn.* **2022**, *60*, 2587–2607. [CrossRef]
12. Ma, X.; Wang, P.; Xu, J.; Xu, J.; Chen, R. Effect of rail straightening irregularity on vertical dynamic characteristics of vehicle-turnout coupling system. *J. Southwest Jiaotong Univ.* **2017**, *48*, 1942–1950.
13. Chang, W.; Cai, X.; Wang, Q.; Tang, X.; Sun, J.; Yang, F. The Influence of track irregularity in front of the turnout on the dynamic performance of vehicles. *Appl. Sci.* **2022**, *12*, 4169. [CrossRef]
14. Zakeri, J.; Esmaeili, M.H.; Mazraeh, A.; Shadfar, M. Impact of heavy urban rail vehicles running over light rail turnouts. *Proc. Inst. Mech. Eng. Part F J. Rail Rapid Transit* **2021**, *235*, 300–312. [CrossRef]
15. Chen, M.; Luo, Y.Y.; Zhang, B. Dynamic characteristic analysis of irregularity under turnout by vehicle-Turnout rigid-Flexible coupling model. *Adv. Mater. Res.* **2014**, *945*, 591–595. [CrossRef]
16. Björn, A.P. A parameterized turnout model for simulation of dynamic vehicle-Turnout interaction with an application to crossing geometry assessment. *Adv. Dyn. Veh. Roads Tracks* **2020**, *8*, 351–358.
17. Chiou, S.B.; Yen, J.Y. Modeling of railway turnout geometry in the frog area with the vehicle wheel trajectory. *Proc. Inst. Mech. Eng. Part F J. Rail Rapid Transit* **2018**, *232*, 1598–1614. [CrossRef]
18. Sun, X.; Wang, P.; Chen, J.Y.; Hao, C.J.; Xu, J.M. Analytical representations of inherent structural irregularities in turnout crossing with moveable point. *Veh. Syst. Dyn.* **2022**, *12*, 1086–1104. [CrossRef]
19. Zhou, C.; Chi, M.; Liang, S.; Wu, X.; Jiang, Y.; Wu, L. Dynamic Behavior Analysis of Urban Light Rail Low Floor Train with Different Wheelset Passing Turnout Area. *J. Mech. Eng.* **2019**, *55*, 98–106. [CrossRef]
20. Zhai, W.M. *Vehicle-Track Coupled Dynamics*; Science Press: Beijing, China, 2015.

Disclaimer/Publisher's Note: The statements, opinions and data contained in all publications are solely those of the individual author(s) and contributor(s) and not of MDPI and/or the editor(s). MDPI and/or the editor(s) disclaim responsibility for any injury to people or property resulting from any ideas, methods, instructions or products referred to in the content.